ISR-BT/AK/EEK 26th February, 1971

ISR RUNNING-IN

Runs 22, 23, 24, 25 on February 12, 15 and 17, 1971

1. General

These runs were made with 4 bunches, and the central field values of the ISR for both rings were (field display):

$B_o \equiv 15.343$ GeV/c

$B_o \equiv 22.467$ GeV/c (Run 25 from about 21.15 h.)

The value of B_o for the nominal 22 GeV/c transfer momentum was adjusted experimentally until the average beam positions in the ISR were the same as at 15 GeV/c, namely $\langle r_F \rangle \approx -40$ mm and $\langle r \rangle \approx -33$ mm. The optimisation of the injection parameters at 22 GeV/c, starting from initial beam transfer settings which had been scaled up from 15 GeV/c proved to be fast and easy. The final beam positions on the luminescent screens after optimizing the injection at 22 GeV/c were within a few mm the same as at 15 GeV/c. The present report deals only with measurements made at 15 GeV/c. The report on run 26 will discuss the adjustment of injection at 22 GeV/c.

2. Reference values for injection at 15 GeV/c and $\langle r_F \rangle = -40$ mm

In these runs we have optimized injection into the two rings at 15 GeV/c by adjustment of all parameters for minimum coherent oscillations around the injection closed orbit.

The following tables list the values which were found and which can be used as reference values for injection with $B_o = 15.343$ GeV/c.

a) Inflectors

	Ring 1	Ring 2
PFN voltages	26.5 kV	26.5 kV
Girder positions	-8.5 mm radial -1 mm vertical	-19 mm radial 0 vertical

b) Settings of BT magnets

The settings of the DAC's of all BT magnets are given in Appendix 1. These figures should be taken as starting values for the DAC settings at the beginning of the run, after which small adjustments with the steering magnets should be made until the beam positions on the screens are approximately as given in c).

c) Beam Observations

After adjustments we should have on the five last screens of the BT channels :

	Ring 1 (TT2)			Ring 2 (TT1)		
	Screen	Radial,	Vertical	Screen	Radial,	Vertical
	LS349	0	0	LS449	0	0
Upstream Septum	LS351	8 L	2 D	LS451	2 L	2 D
Downstream Septum	LS352	3 L	2 D	LS452	3 R	1 D
Upstream Kicker	LS7175	6 R	0	LS2485	7 L	0
Downstream Kicker	LS7174	8 R	0	LS2486	7 L	0

Ideally the numerical values of the radial positions given in the Table should be the same for the two Rings, but with L(left) and R (right) interchanged. The difference between the two Rings can be attributed to closed orbit distortions which are different in the two Rings. The same remarks apply to differences between the two Rings in Table a) and to non-zero vertical positions in Table c).

3. Remarks on PS momentum in Run 23

In run 23, after optimizing injection into the two rings,we have obtained on the two last screens of the transfer channels (Up- and Downstream of the inflectors) the following beam positions:

	Ring 1			Ring 2	
	Radial,	Vertical		Radial,	Vertical
LS7175	+ 3	0	LS2485	- 4	0
LS7174	+ 5	0	LS2486	- 4	0

with the girder positions of - 8.5 mm and -19 mm for Ring 1 and Ring 2 respectively.

If we compare these observations with the reference values given in section 2, we see that for both Rings the beam was displaced 3 mm towards the centre of the ISR. We attribute this difference to the fact that during Run 23, due to an error in radial position of the beam in the PS at the moment of ejection, the momentum of the ejected protons was 0.13% lower than usual.

The same 3 mm displacement is also visible in Fig. 1 which shows, for both Run 20 and Run 23, the percentage of coasting beam remaining after horizontal movement of the inflector in Ring 1, starting from the same girder position - 8.5 mm at injection.

The two curves shown in Fig. 1 are very similar, which means that the shape of a beam coasting on the injection orbit is reproducible from one run to the next.

4. Measurements made in Ring 2 (Run 23)

a) Horizontal movement of inflector 248

Figures 2, 3 and 4 show the percentage of protons in a coasting beam which survive if the inflector with the shutter closed is displaced horizontally. These figures and also Fig.1 were measured without sextupoles and without R.F. The only difference between the three figures is the position of the inflector while the single shot was injected.

The horizontal coordinate in all these figures is the "girder position" G. This is defined as the position of the shutter edge on the side of the stack,with respect to the central orbit, at the exit of the downstream inflector magnet. The geometry is shown in Fig. 5. The aperture limitation on the side of the inflector yoke is given by the return conductor and occurs at r = (G - 52.5)mm. For a beam coasting on the injection orbit the aperture limitation caused by the shutter at the inflector exit is r = (G - 2) mm, since the shutter is 2 mm thick. However, the two inflector magnets are aligned along the nominal trajectory of the injection beam assuming total deflection of 2.6 mrad in the inflector. The latter has a total length of almost 4 m and therefore the upstream end of the upstream inflector magnet is 5 mm further away from the central orbit than the downstream end of the downstream inflector magnet. As a consequence the aperture limitation on the shutter side occurs at the inflector entrance and is at r = (G - 7)mm. The window in the inflector seen by a beam coasting on the injection orbit therefore has a width of 45.5 mm.

Some other useful data concerning the geometry at the exit of the downstream inflector magnet are as follows :

- The front edge of the ferrite core is at r = (G - 8) mm.
- The edge of the good field region is at r = (G - 11) mm
- The cross on the luminescent screen is half-way in between the edges of the good field region and the return conductor, and therefore is at r = (G - 31.75) mm.

At present, with injection without a bump,the deflection in the inflector is about 3.1 mrad and therefore one would expect to see the beam on the upstream LS about 1 mm closer to the inflector yoke than on the downstream LS. The data in the Table given under 2c) tend to confirm this tendency but it should be remembered that closed orbit errors and mechanical alignment errors can easily account for discrepancies of 1 mm.

Returning now to Figures 2, 3 and 4 we see that they are practically identical. The two curves in Fig. 3 represent two different measurements made under the same conditions with an interval of half an hour in between and show that the measurements are very reproducible. The similarity of Figures 2 to 4 could of course be expected since the size and position of the coasting beam should not be affected by the inflector position as long as the beam does not touch the inflector. All curves indicate that the coasting beam has a low energy tail. When the inflector is moved towards the central orbit, this tail is the first to be absorbed and causes the dip in the region G = -17.5 mm. When the inflector is moved away from the central orbit the low energy tail is the last to be absorbed. This asymmetrical beam size has also been drawn schematically in Figure 5.

If we centre the inflectors on the solid curve in Fig. 1 and the curves of Figures 2 to 4, disregarding the low energy tail,we find G = -8.5 mm for Ring 1 and G = -19 mm for Ring 2. As mentioned in para.3 the beam is normally about 3 mm closer to the central orbit. It seems a reasonable compromise to use nevertheless the girder position just mentioned so that then there is somewhat more room for the low energy tail. Looking at Fig. 10 (see below) we see that also with RF and sextupoles on, G = -8.5 mm is a reasonable girder position for Ring 1.

It is difficult to make quantitative statements about the emittance of a beam with such a low energy tail. However, as a rough approximation, we can make the following exercise.

If we first consider the r.h.s. of the curves it looks as if the low energy tail contains about 5% of the protons. We disregard these 5% and interpret the change in G required to go from 90% to 0% surviving beam as the beam half width w corresponding to an emittance which contains 95% of the protons. We then find $w \approx 12$ mm. The low energy tail on the l.h.s. of the curves seems to be larger and to contain more protons than would be guessed from the dip to the right of G = 17.5 mm. However, it may also contain "normal" protons which lost energy by passing through a short part of the shutter when the inflector is moved away from the central orbit. We disregard this tail and extrapolate the curves down to zero with the dotted curve which has the same shape as the r.h.s. The value of w found from the inflector displacement between 95% and 0% of surviving beam is then about 13 mm. Since at the inflector $\beta_H \approx 37$ m this then gives a horizontal emittance of about $E_H \approx \frac{(12.5)^2}{37}\pi = 4.2\pi$ mm x mrad and this figure is several times larger than would be expected from the beam emittances measured with the SEM's in the transfer channels and in the Rings.

b) Vertical closed orbit in inflector 248

Figure 6 shows the percentage of coasting beam remaining after vertical movement of the inflector in Ring 2. When injecting we had placed the inflector at z = 0 mm. Comparing the left and right hand side slope of the curve one sees that the vertical c.o. in the inflector is at z = + 0.1 mm. The accuracy of the measurements of the displacement is of the order of 0.1 mm and therefore the inflector position z = 0 mm will be retained for Ring 2.

The loss in circulating beam is 5% for

$z = -6$ mm

$z = +6.1$ mm.

The effective vertical aperture of FK is about 19 mm. The results therefore indicate a vertical beam size in FK of 19 - 12.1 = 6.9 mm, corresponding to an emittance

$$\hat{z}^2/\beta_v = (3.45)^2/14 = 0.85 \text{ mm x mrad.}$$

5. Influence of RF and sextupoles (Run 24)

It had been found by the RF group during previous runs, that the size of the beam coasting on the injection orbit was apparently increased by the RF voltage and that this effect could be stabilized by means of sextupoles. Therefore during run 24 some measurements were made on Ring 1 to obtain more quantitative information about this effect.

Figure 7 shows the percentage of surviving beam on the injection orbit, as a function of G, without RF and without sextupoles, for the so-called "bare machine". It has the same shape as the two curves in Fig. 1 and falls about half-way in between these two. Figures 1 and 7 therefore give an idea of the variation of the PS ejected beam from one run to the next.

Figure 8 shows the same measurements with the p f w and sextupoles adjusted to the working point "Cleo". The curve is very similar to that of Fig. 7 so that under these conditions the sextupoles have very little effect.

Figure 9 shows the same measurement with the bare machine, but with the RF turned on at constant frequency and holding the beam bunched on the injection orbit. Under these conditions the beam is clearly much larger and as soon as the inflector is moved a bit from its initial position it scrapes off the beam .

Fig. 10 shows a measurement with working point "Cleo" and with RF on. The beam is now only a few mm wider than in the case of Fig. 7 (remember that a wide beam corresponds to a narrow curve in the Figures) and the curve of Fig. 10 still has a comfortable plateau around the region G = -8.5 mm. The low energy tail in Fig. 10 is much smaller than in the other figures, because the RF removes the low energy protons from the coasting beam.

The working point "Cleo" is defined by the following parameters

a)	Pole face windings	$\Delta Q_H = 0.014$
		$\Delta Q_V = -0.038$
b)	Terwilliger	TD1 = 0%
c)	Sextupoles	SF = 9%
		SD = 3.3%

A. Knezovic

B. de Raad

Distribution

Parameter Committee

Running-in-Committee

Engineers-in-Charge

BT Group Scientific Staff

E. Brouzet - MPS

P. Höffert - DI/HP

Appendix 1: List of recommended DAC settings for sections 1,2,3 and 4 at 15 GeV/c. The HB403 value is for the d.c. supply only.

0101	QF101	+0.2318
0102	HB101	+0.25778
0103	QD102	+0.2636
0104	VB101	+0.30960
0105	QF103	+0.2208
0106	HB102	+0.22729
0107	QD104	+0.2292
0110	QF105	+0.1909
0111	HB103	+0.19320
0112	VB102	+0.31300
0113	QD106	+0.2698
0114	QF107	+0.2144
0201	QD208	+0.2534
0202	QF209	+0.26704
0203	QD210	+0.29332
0204	QF211	+0.27078
0205	QD212	+0.18418
0206	QF213	+0.22803
0207	QD214M	+0.3376
0210	QF215M	+0.3315
0211	VS201	+0.00030
0212	HS202	+0.00030
0213	VS202	+0.00030
0302	QD332M	+0.3758
0303	HB301	+0.00757
0304	QF333M	+0.3693
0305	VB303M	+0.35614
0306	HB332	+0.24346
0307	QD346	+0.3143
0310	VB307	+0.20830
0311	QF347	+0.2372
0312	QD348	+0.24830
0401	VB308	+0.28975
0402	QF349	+0.2323
0403	HB333	+0.13909
0404	VB309	+0.26986
0405	QD350	+0.2665
0406	QF351	+0.26370
0407	HB334	+0.12791
0410	VHB 301M	+0.48821
0501	HB403	+0.3160
0503	QD408M	+0.3727
0504	QF409M	+0.3713
0505	HB404M	+0.3953
0506	HB421C	+0.00030
0507	HB423C	+0.00100
0604	HB428M	+0.36840
0605	VB403M	+0.35668
0606	HB432	+0.03694
0607	QD446	+0.3232
0610	VB407	+0.20452
0611	QF447	+0.2464
0612	QD448	+0.27660
0701	VB408	+0.28743
0702	QF449	+0.2490
0703	HB433	+0.11481
0704	VB409	+0.27257
0705	QD450	+0.2668
0706	QF451	+0.26430
0707	HB434	+0.06634
0710	VHB401M	+0.48852

Le 15-2-1971
Run 23

Percentage of cooling beam = f(x)
FKI (Ring 1)

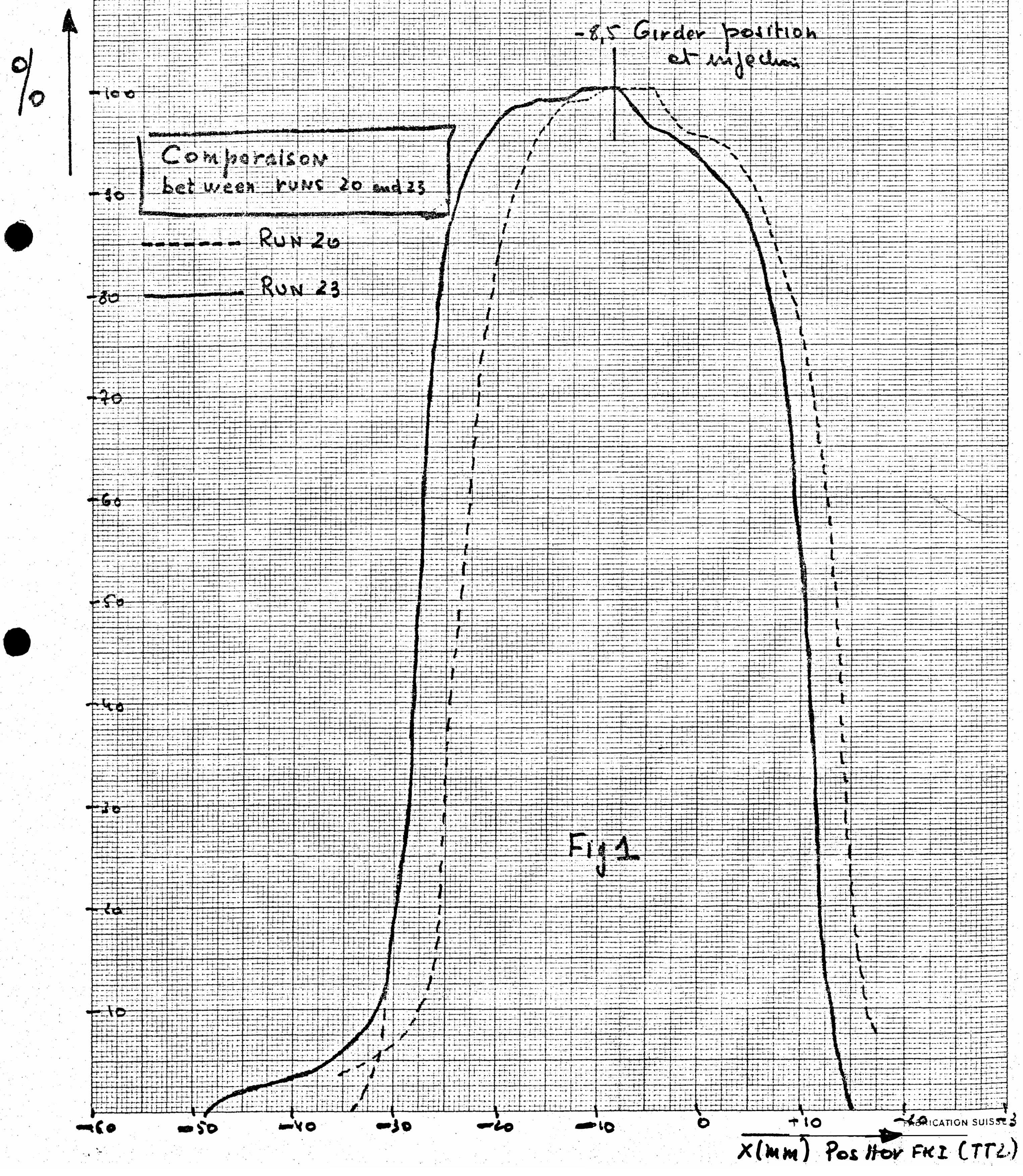

Fig 1

Le 15-2-1971
Run n°23

Percentage of coasting beam = f(x) FKI (Ring 2)

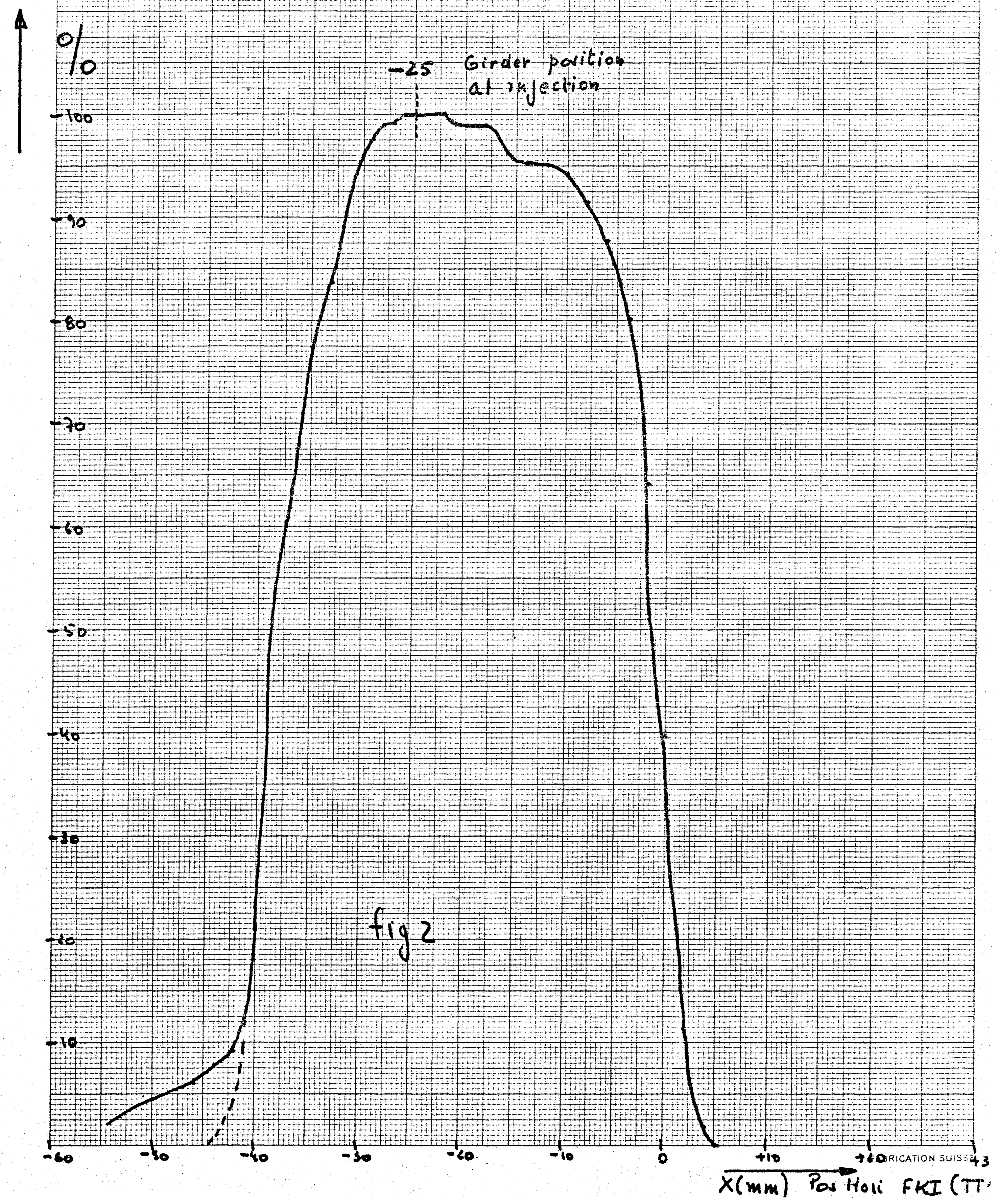

Le 15-2-1971

Percentage of coasting beam = f(x)

(Ring 2)

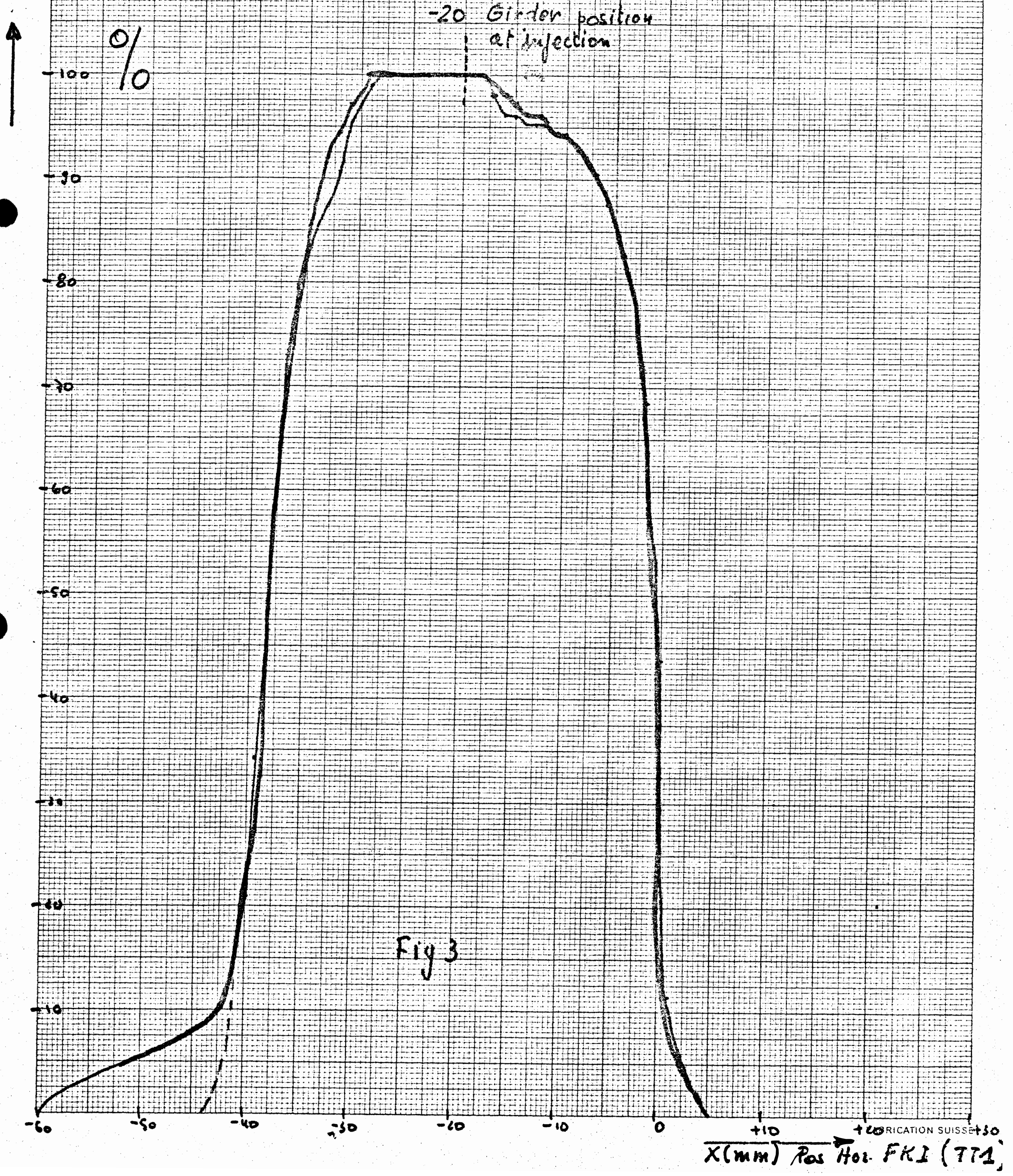

Fig 3

Le 15-2-1971
Run n° 23

Percentage of coasting beam = f(x) FKI (Ring 2)

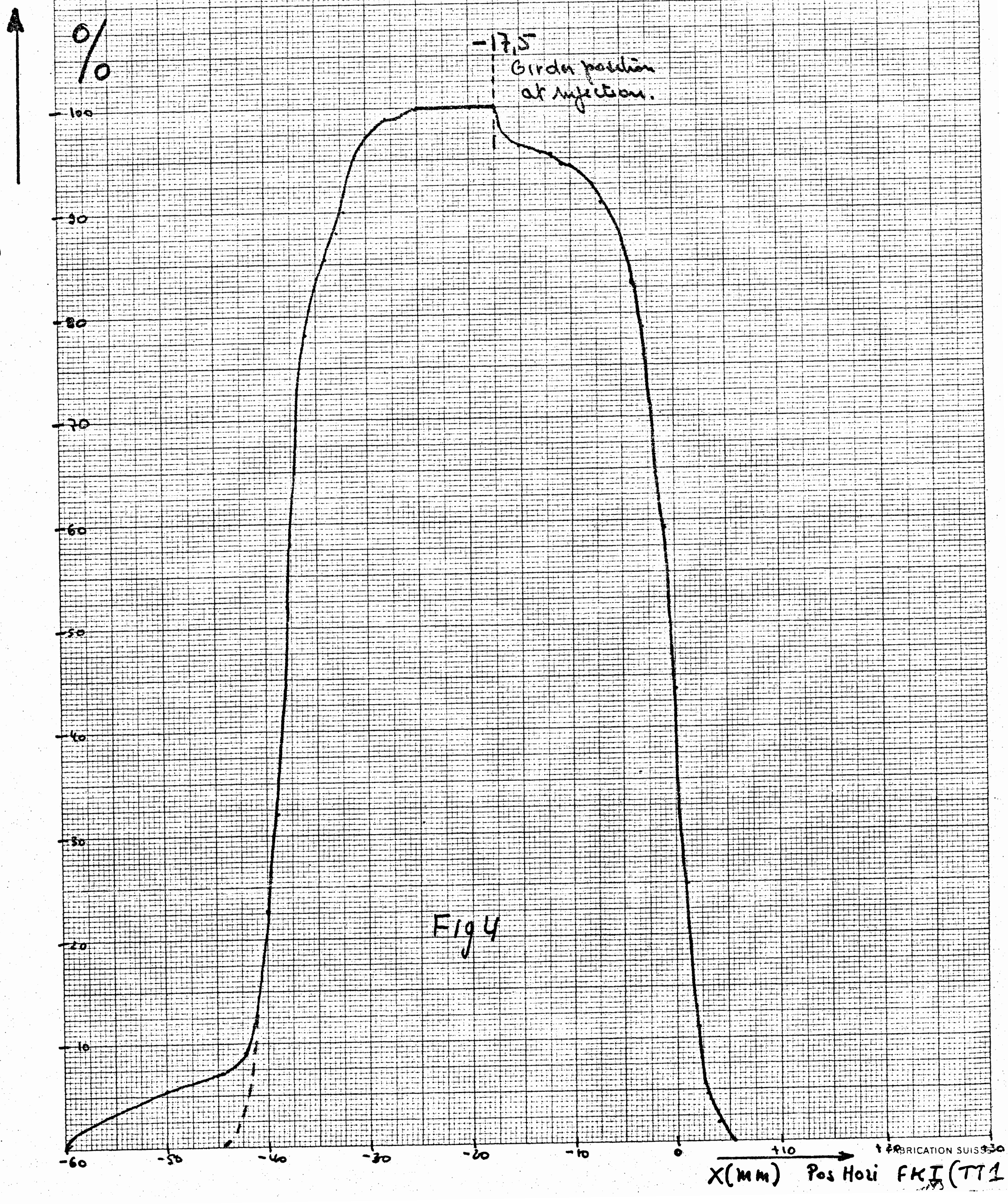

Fig 4

Geometry of Injection (LS 2486)

(Ring 2.)

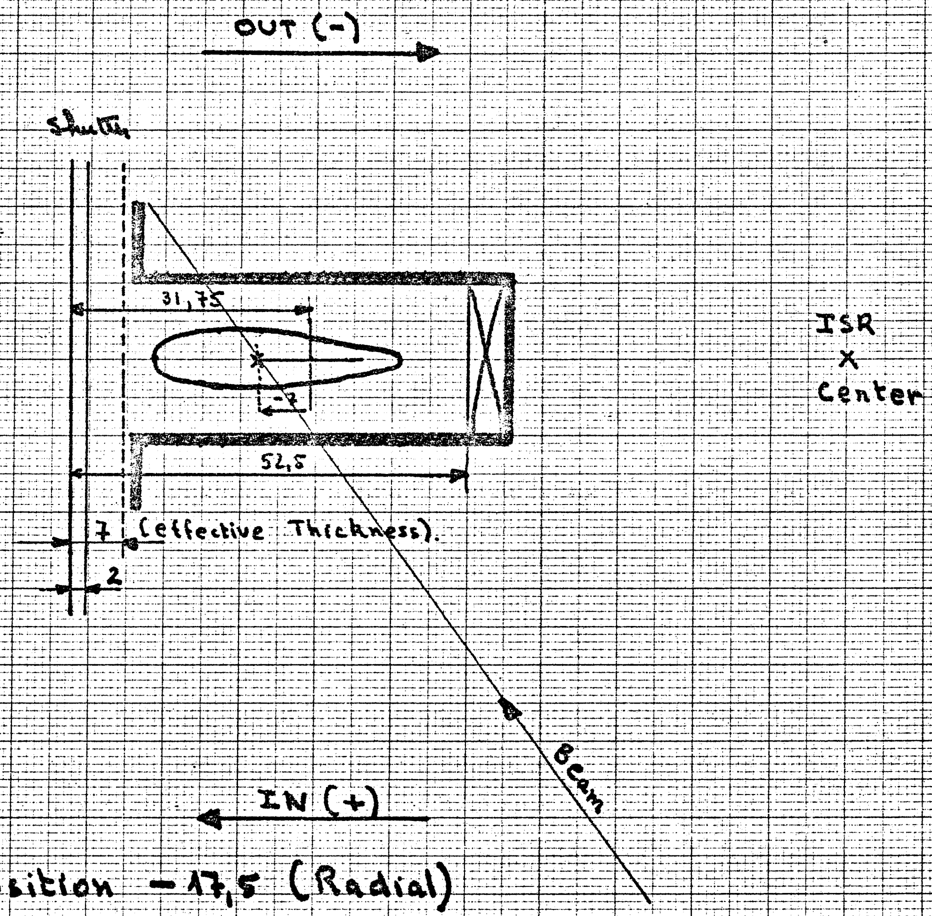

Girder position -17,5 (Radial)

(Fig 5)

Le 15-2-1971
Run no23

Percentage of coasting beam = f(z)
FKI (Ring 2)

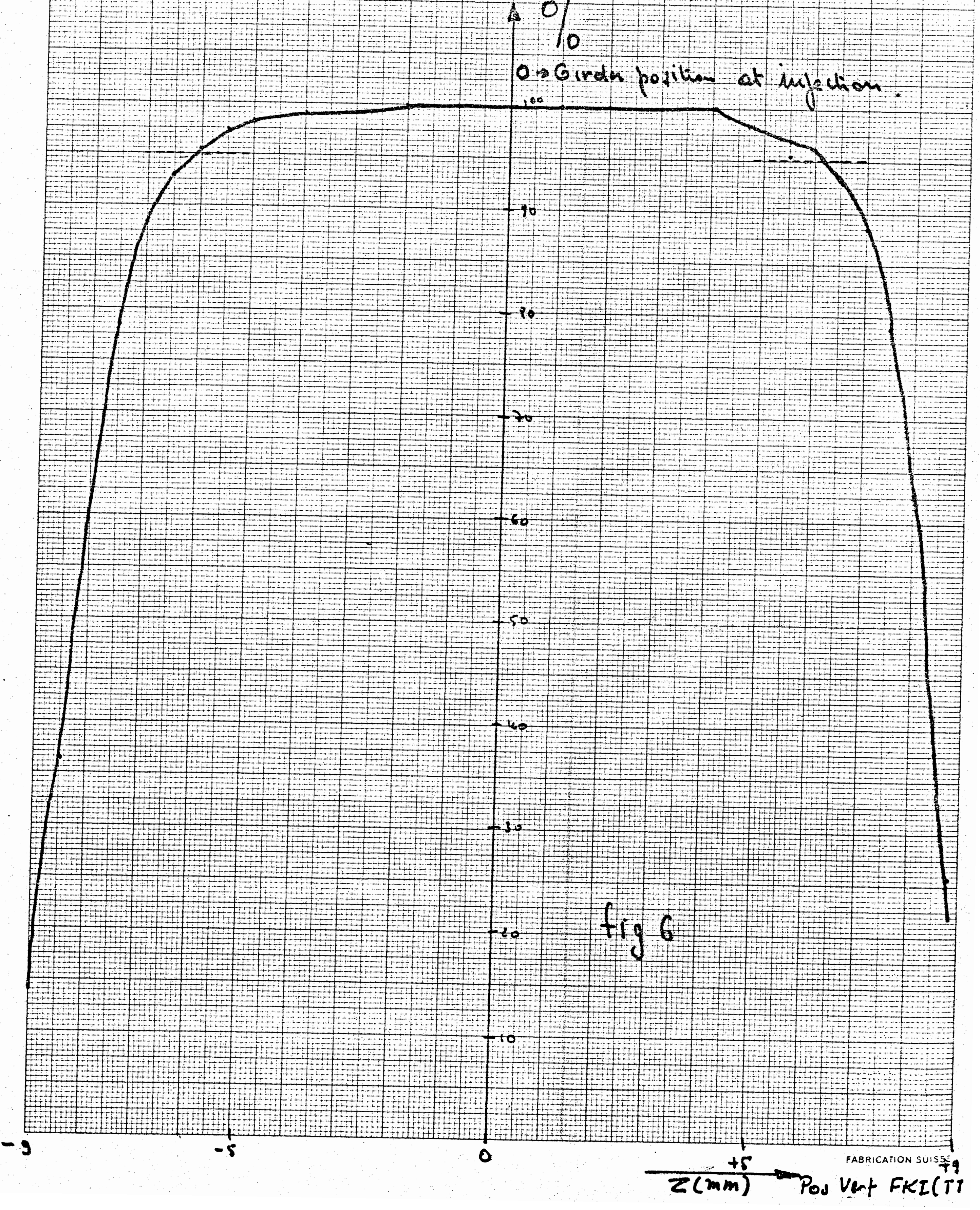

fig 6

Leitz - 2 - 1971
Run 24

Percentage of coasting beam = $f(x)_{FKI}$ (Ring 1).

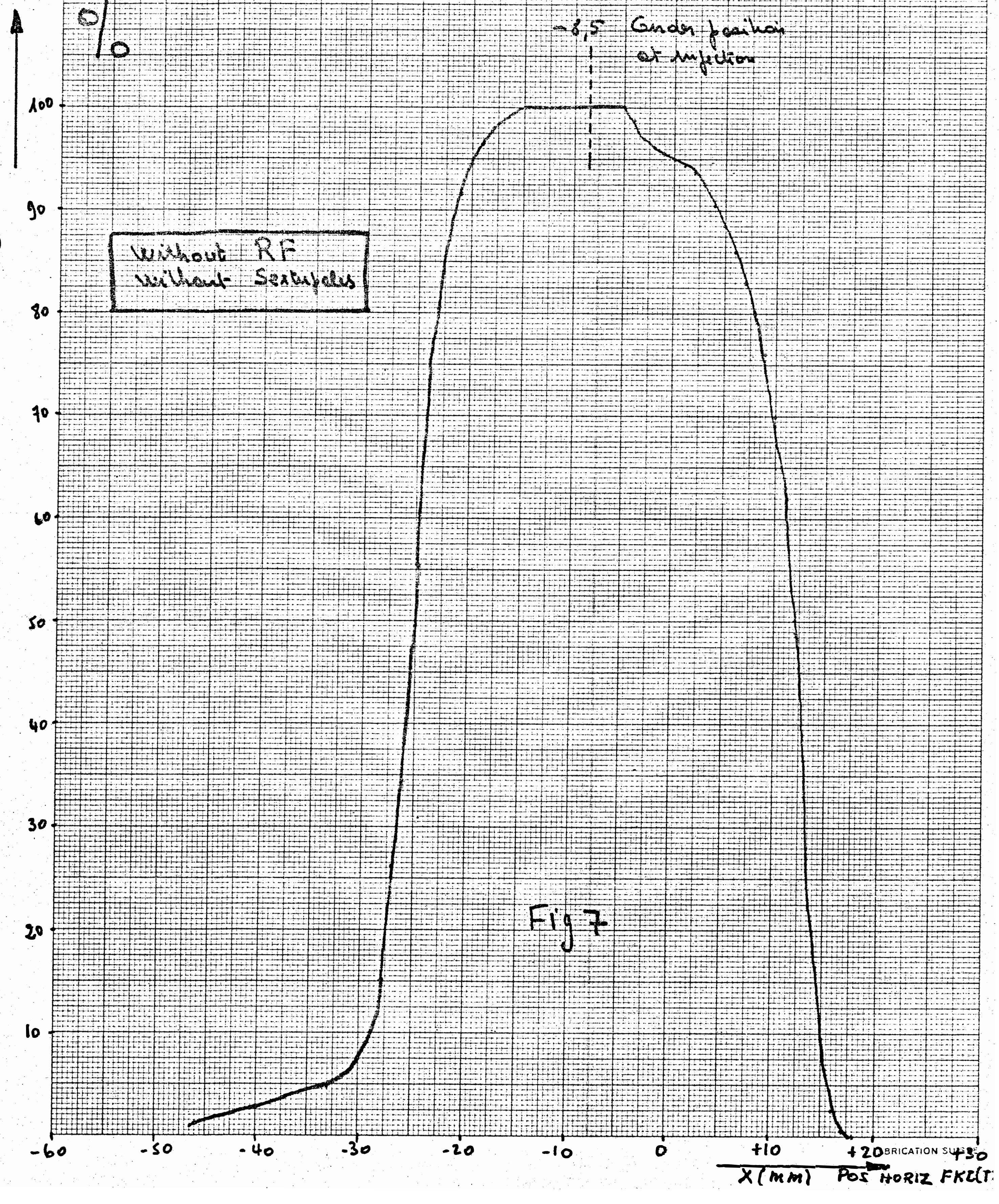

Fig 7

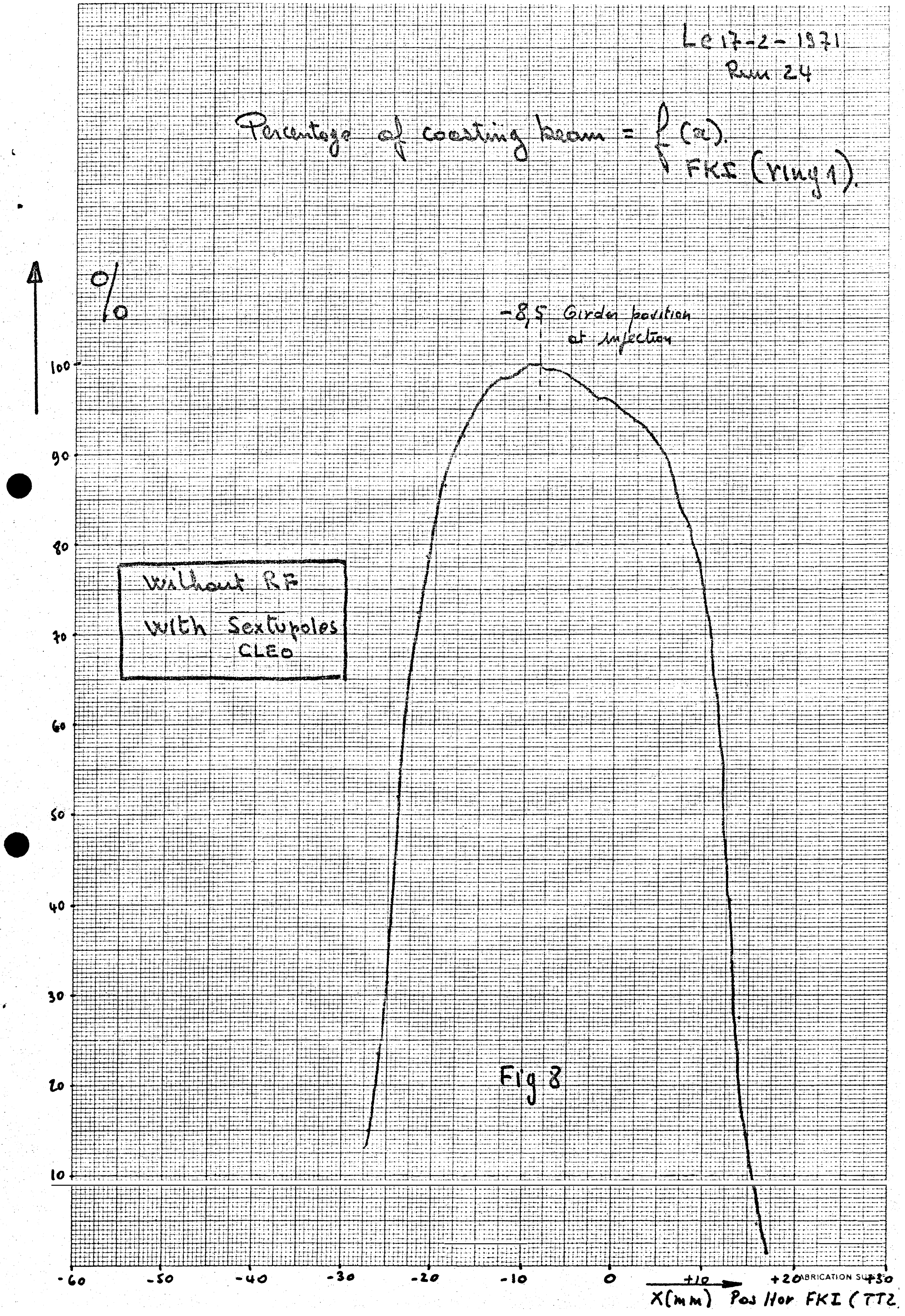
Le 17-2-1971
Run 24
Percentage of coasting beam = f(x).
FKI (ring 1).
%
-8,5 Girder position
at injection
100
90
80
70
60
50
40
30
20
10
without RF
with Sextupoles
CLEO
Fig 8
-60
-50
-40
-30
-20
-10
0
+10
+20
+30
X(mm) Pos Hor FKI (TT2

Le 17-2-1971
Run 24

Percentage of coasting beam = f(x)
FKI (Ring 1)

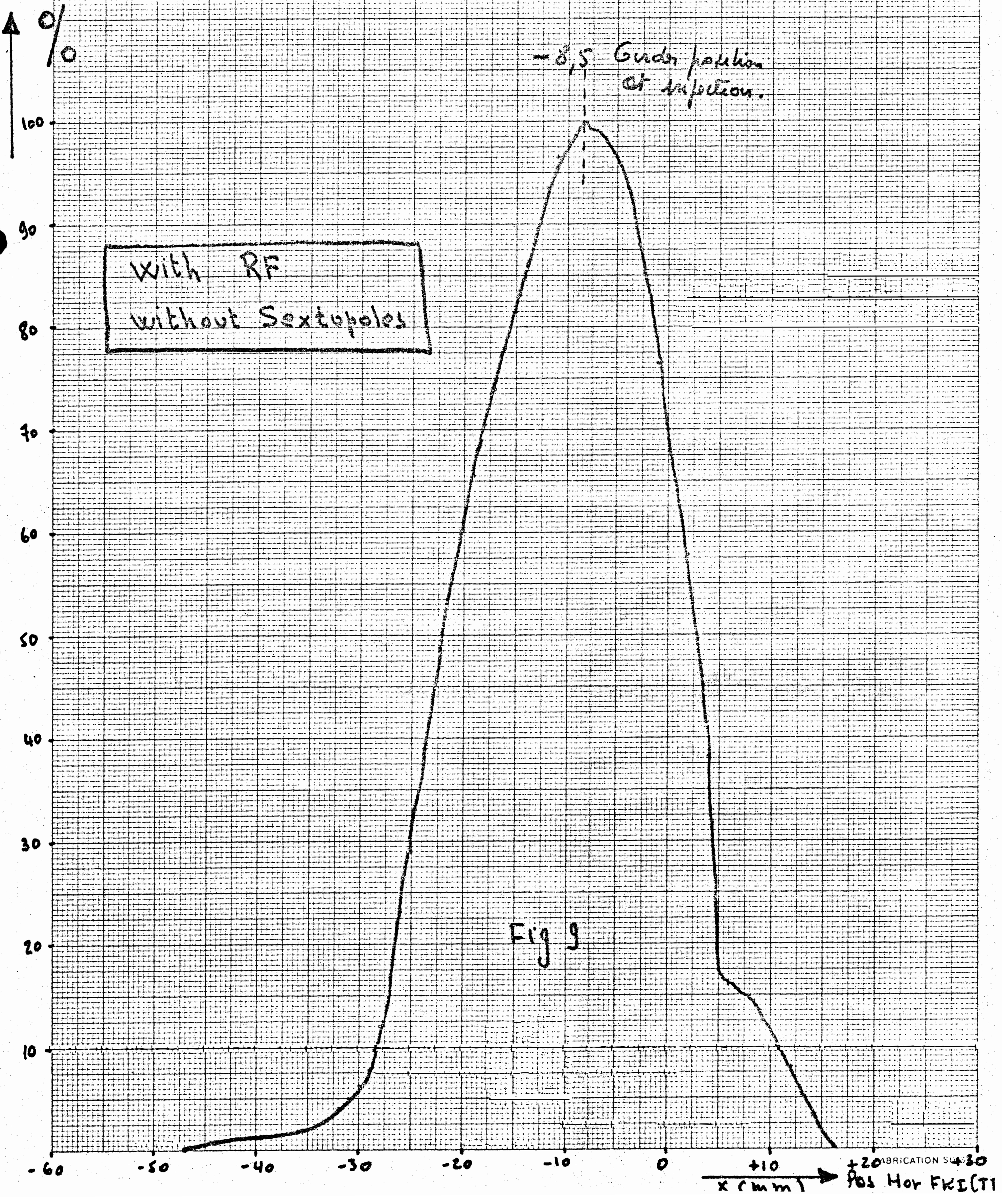

Fig 9

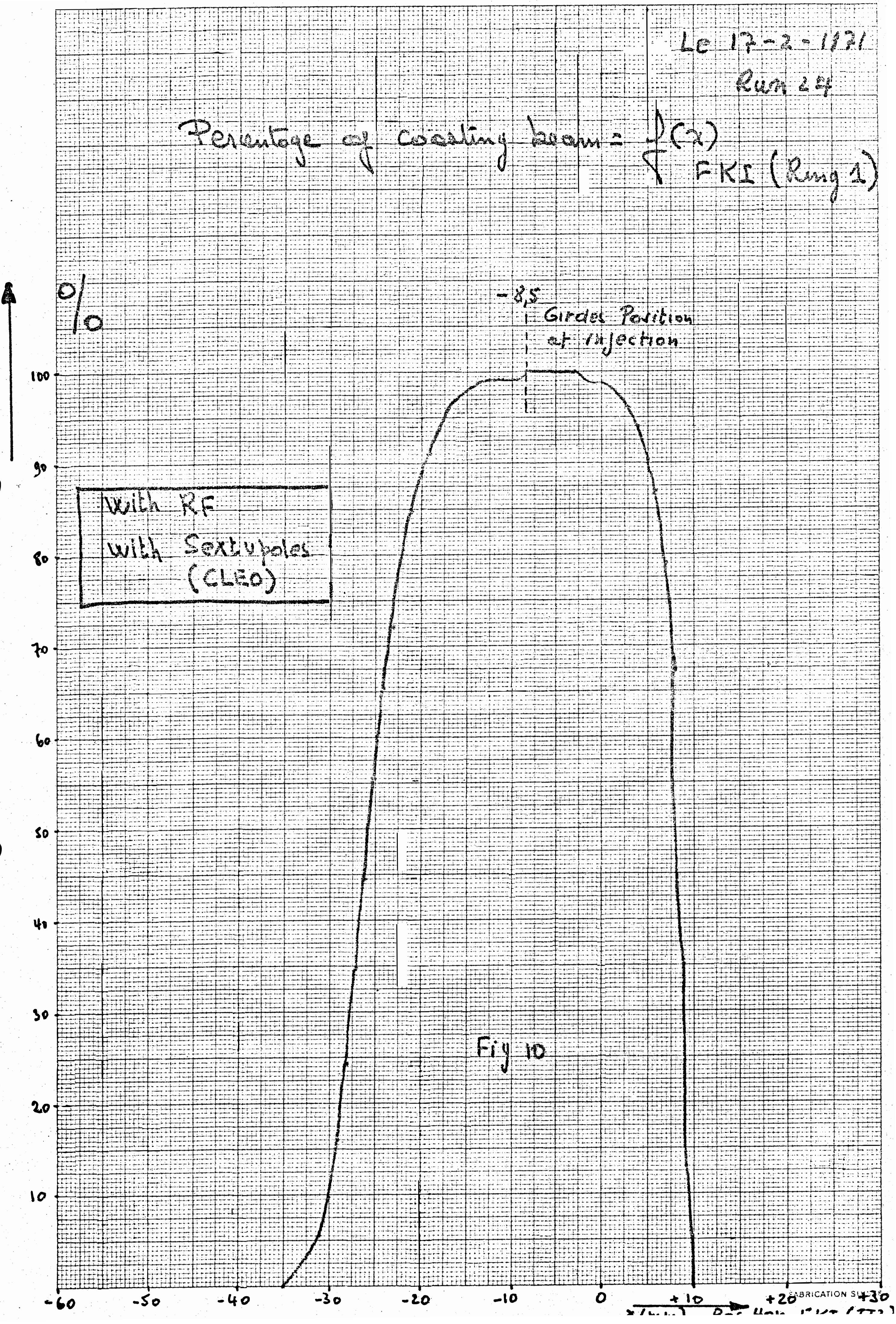
Le 17-2-1971
Run 24
Percentage of coasting beam = f(x)
FKI (Ring 1)
%
-8,5
Girder Position
at injection
with RF
with Sextupoles
(CLEO)
Fig 10
100
90
80
70
60
50
40
30
20
10
-60
-50
-40
-30
-20
-10
0
+10
+20
+30